Limnol. Oceanogr., 49(5), 2004, 1884–1895

Denitrification and hydrologic transient storage in a glacial meltwater stream, McMurdo Dry Valleys, Antarctica

Michael N. Gooseff[1] *and Diane M. McKnight*
Institute of Arctic and Alpine Research, University of Colorado, Boulder, Colorado 80309

Robert L. Runkel
U.S. Geological Survey, Mail Stop 415, Denver Federal Center, Denver, Colorado, 80225

John H. Duff
U.S. Geological Survey, Mail Stop 439, Menlo Park, California 94025

Abstract

In extreme environments, retention of nutrients within stream ecosystems contributes to the persistence of aquatic biota and continuity of ecosystem function. In the McMurdo Dry Valleys, Antarctica, many glacial meltwater streams flow for only 5–12 weeks a year and yet support extensive benthic microbial communities. We investigated NO_3^- uptake and denitrification in Green Creek by analyzing small-scale microbial mat dynamics in mesocosms and reach-scale nutrient cycling in two whole-stream NO_3^- enrichment experiments. Nitrate uptake results indicated that microbial mats were nitrogen (N)-limited, with NO_3^- uptake rates as high as 16 nmol N cm^{-2} h^{-1}. Denitrification potentials associated with microbial mats were also as high as 16 nmol N cm^{-2} h^{-1}. During two whole-stream NO_3^--enrichment experiments, a simultaneous pulse of NO_2^- was observed in the stream water. The one-dimensional solute transport model with inflow and storage was modified to simulate two storage zones: one to account for short time scale hydrologic exchange of stream water into and out of the benthic microbial mat, the other to account for longer time scale hydrologic exchange with the hyporheic zone. Simulations indicate that injected NO_3^- was removed both in the microbial mat and in the hyporheic zone and that as much as 20% of the NO_3^- that entered the microbial mat and hyporheic zone was transformed to NO_2^- by dissimilatory reduction. Because of the rapid hydrologic exchange in microbial mats, it is likely that denitrification is limited either by biotic assimilation, reductase limitation, or transport limitation (reduced NO_2^- is transported away from reducing microbes).

Dry valley glacial meltwater streams are simple physical systems, ideal for studying stream-hyporheic biogeochemical interactions. There is no contribution to stream flow from precipitation (either directly or from snowmelt), and there are no hillslope additions of water or solutes. Further, the hyporheic zones are well defined, bounded at depths of 0.4 to 0.7 m by permafrost, extending several meters from stream edges (Gooseff et al. 2003). In these streams, hyporheic zone exchange and biotic assimilation are important controls on biogeochemical cycling. At the mineral grain scale, Maurice et al. (2002) recently documented weathering processes occurring in the hyporheic zone of a dry valley stream at rates higher than typically found in temperate watersheds, as well as the presence of denitrifying bacteria. Similarly, at the reach scale, Gooseff et al. (2002) have shown that hyporheic exchange controls inorganic weathering product solute loads to lakes. Previous work by Howard-Williams et al. (1989, 1997), Vincent et al. (1993*a*), and McKnight et al. (2004) has shown that stream benthic microbial mats exert a significant control on stream nutrient cycling at the mat and stream reach scales. McKnight et al. (2004) noted the presence of a low but well-defined NO_2^- pulse during a whole-stream NO_3^- tracer enrichment experiment in Green Creek, which they attributed to nitrate reduction during denitrification within hyporheic sediments. Vincent et al. (1993*a*) detailed strong negative gradients of dissolved oxygen (DO) coinciding with positive chlorophyll *a*, nutrient, and photosynthesis gradients (with depth) within dry valley benthic microbial mats ranging from 1 mm to 20 mm in thickness, suggesting the potential for denitrification processes within benthic microbial mats.

Several microbial processes contribute to nitrogen (N) transformations in streams depending on the oxidation/reduction processes occurring in the stream/hyporheic habitat. Denitrification is the sequential reduction of NO_3^- to NO_2^-, then to N_2O, and finally to N_2 (Knowles 1982). Denitrification preferentially occurs in reducing, anoxic environments; therefore, it occurs at low rates in oligotrophic streams because high DO concentrations provide an abundant and energetically favorable electron acceptor during organic matter oxidation. Denitrification in the hyporheic zone and stream sediments is a significant sink for NO_3^- in some streams (Hill 1979; Holmes et al. 1996; Valett et al. 1996), but is

[1] To whom correspondence should be addressed. Present address: Department of Aquatic, Watershed and Earth Resources, Utah State University, Logan, Utah 84322-5210 (michael.gooseff@usu.edu).

Acknowledgments

We thank L. Scott, J. Sheets, M. Hodges, L. Williams, K. Lewis, P. Langevin, K. Van Gelder, and A. Bomblies for assistance in the field; D. Niyogi for help in designing the denitrification experiment; H. Taylor and T. Plowman for use of analytical instruments; and C. Seibold and M. Williams for assistance with sample analysis. K. Bencala, J. Harvey, and K. Nydick provided valuable comments on earlier versions of this manuscript. This work was supported by the NSF Office of Polar Programs (grant 9813061).

less significant in others (Martin et al. 2001). Intermediate species in the denitrification pathway (NO_2^- and N_2O) have been observed in hyporheic zone pore waters (Duff and Triska 1990) and in chamber or column experiments using hyporheic sediments (Stief et al. 2002; Sheibley et al. 2003) but have not been reported in stream waters for most whole-stream nitrate enrichment experiments (e.g., Triska et al. 1989; Kim et al. 1992). This result indicates that there was no reductase limitation (all necessary microbes are immediately available for sequential N reduction) nor transport limitation (exchange of solutes faster than reaction time scales) within the experimental stream and/or hyporheic microbial communities. Recently, Stief et al. (2002) found that NO_2^- produced by subsurface denitrification was only evident in surface waters when overlying waters were hypoxic. Transport limitation could become more important in extreme environments with relatively rapid rate of hydrologic exchange and limited rates of microbial processes.

The ability of benthic microbial mats, periphyton, and macrophytes to slow and distort near-bed velocity profiles has been addressed in several temperate stream settings (Kim et al. 1990; Sand-Jensen and Mebus 1996; Wilcock et al. 1999; Dodds and Biggs 2002) and laboratory settings (Mulholland 1994; Nikora et al. 2002). In particular, Kim et al. (1992), Mulholland et al. (1994), and Wilcock et al. (1999) suggest that benthic biota provide a transient storage zone with characteristics distinct from main channel stream flow. DeAngelis et al. (1995) proposed a transient storage model based on stream hydraulics as altered by periphyton. Dent and Henry (1999) took that model a step further by including hyporheic exchange to investigate stream periphyton dependence on subsurface N cycling. Choi et al. (2000) found that multiple storage zone models were useful when multiple time scales of exchange could be clearly identified (i.e., when strongly differing solute fluxes could be identified) in stream tracer experiments. We propose that multiple transient storage zones, defined by (1) hyporheic exchange and (2) benthic boundary layers formed by microbial mats, are important in dry valley stream N cycling.

In this study, we hypothesize that denitrification reactions occur rapidly in hyporheic zone sediments and in benthic microbial mats of dry valley glacial meltwater streams. Microcosm experiments were used to characterize potential NO_3^- uptake by algae and potential denitrification rates associated with the microbial mats and sediments. In addition, we used simulations from two whole-stream tracer experiments in Green Creek to estimate rates of NO_3^- conversion to NO_2^- by the benthic communities. We conclude that the rapid NO_3^- removal that occurs on the time scale of streamwater advection, by algae and denitrification, is more likely to occur in the hydrologic transient storage zone created by benthic microbial mats than in the hyporheic zone.

Site description—The McMurdo Dry Valleys are located at roughly 78°S latitude, on the western coast of McMurdo Sound, Antarctica (Fig. 1). Glaciers, open expanses of barren patterned ground, stream channels, and permanently ice-covered, closed basin lakes dominate the landscape. Soils contain cryptobiotic rotifers, tardigrades, and nematodes but lack terrestrial vegetation. The climate is defined by a mean

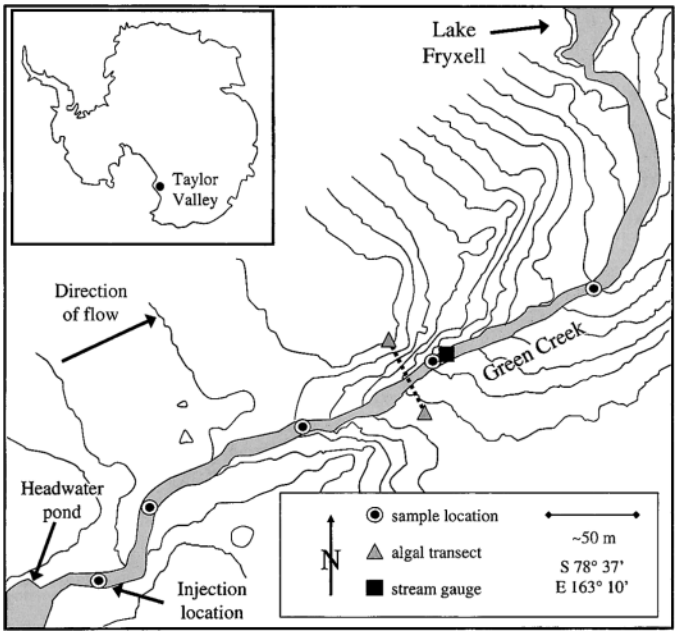

Fig. 1. Map of Green Creek sampling locations and location map of the Dry Valleys in the inset. Contour interval is 1 m.

annual air temperature of −20°C, less than 10 cm water equivalent of precipitation, as snow, and austral summers with 24-h sunlight.

Glacial melt is the main source of stream flow, which generally lasts for 5–12 weeks during the austral summer. Green Creek (Fig. 1), the site of the experiments reported here, is 0.9 km in length and is one of 13 streams draining into Lake Fryxell in Taylor Valley. Streambeds are composed of porous alluvium, in which extensive hyporheic zones are established, extending several meters from the edge of the stream. Streams exchange water with extended portions of the hyporheic zone over time scales of months, a period that is sufficiently longer than can be identified with stream tracer experiments (Gooseff et al. 2003). In shallow-gradient stream reaches such as Green Creek, freeze–thaw cycles operating over geologic time scales have produced a stable stone pavement, which allows for extensive microbial mat coverage on top of the pavement (McKnight et al. 1998, 1999). Spaces between the rocks composing the stone pavement are generally filled with porous alluvium (Fig. 2).

The benthic microbial mats that occur in the main channel are typically orange colored and are composed of 10 to 15 species of *Oscillatoria* and, predominantly, *Phormidium* (Alger et al. 1997). Black microbial mats occur on the edges of streams, where they are intermittently wet and are mostly composed of one or two *Nostoc* species (Alger et al. 1997; McKnight et al. 1998). Alger et al. (1997) have reported Green Creek benthic *Nostoc* and *Phormidium* biomass levels ranging from nondetection to 60.78 μg chlorophyll *a* cm^{-2} and 3.57 to 10.09 μg chlorophyll *a* cm^{-2}, respectively (n = 5 in each case). Microbial mats are 1–20 mm thick (Vincent et al. 1993*a*). During the winter, the microbial mats remain on the streambeds in a ''freeze-dried'' state and begin photosynthesizing within a few hours at the onset of stream flow

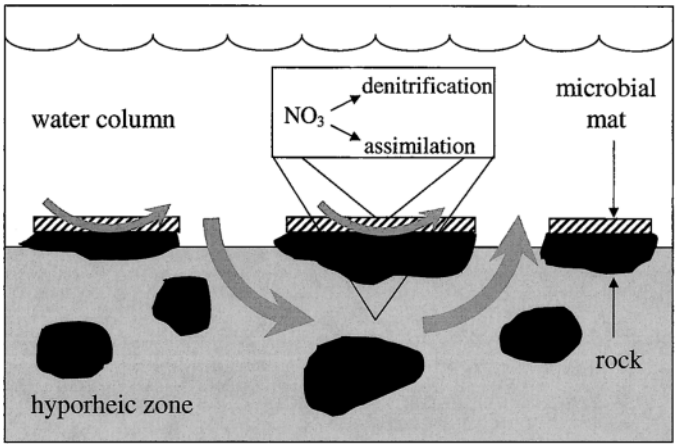

Fig. 2. Conceptual model of stream-water exchange with microbial mats, established on the benthic stone pavement, and the hyporheic zone underneath.

the following summer (Vincent et al. 1993*b*). It has been shown that benthic microbial mats control dissolved nutrient loading to the closed basin lakes through biotic assimilation (McKnight et al. 2004). Sources of nutrients in dry valley streams include over-winter freeze concentration of nutrients in hyporheic zones, atmospheric deposition, autochthonous microbial production, and streambed sediments (Vincent et al. 1993*b*; Howard-Williams et al. 1997).

Materials and methods

Mesocosm experiments—During the 1998–1999 austral summer, orange *Phormidium* spp. dominated microbial mat, black *Nostoc* spp. dominated microbial mat, and streambed sediment samples from Green Creek were assayed for NO_3^- uptake and denitrification potentials. For mat NO_3^- uptake assays, 2-cm–diameter microbial mat samples were cored from *Phormidium* and *Nostoc* mats and added to 250-ml clear glass jars. Alternatively, 10 ml of sediment was added to the jars, and 100 ml of unfiltered stream water were added to each jar. For each substrate, six incubations were run: one unamended control, one unamended control killed with formalin, three amended with 100 ml of 10.7 μmol N L^{-1} KNO_3 solution, and one amended with the KNO_3 solution but killed with formalin. All samples were incubated for 8 h; sediment samples were incubated in the dark and microbial mat samples were incubated in the stream, so they experienced ambient daylight and water temperature. After 2 h, 4 h, and 8 h, 25-ml aliquots were removed from the mesocosms. Water samples were immediately filtered with 1.2-μm GF/C filters and frozen prior to analysis in Boulder, Colorado. Water samples were analyzed for NO_3^- by standard methods using a Dionex model 120 ion chromatograph (Dionex Corporation).

Denitrification potential was measured using the acetylene (C_2H_2) block technique (Tiedje et al. 1989). Fifteen incubations were run for each substrate in 25-ml serum bottles consisting of three replicates each: (1) unamended, (2) amended with glucose, (3) amended with nitrate, (4) amended with NO_3^- plus glucose, or (5) amended with nitrate but killed with formalin. Serum bottles amended with NO_3^- received 10 ml of 10.7 μmol N L^{-1} KNO_3 solution dissolved in stream water; serum bottles amended with glucose received 10 ml of 12.5 μmol C L^{-1} glucose solution dissolved in stream water. All serum bottles were sparged with N_2 gas for 5 min through a syringe canicula, and then 2 ml of C_2H_2 gas was added. The serum bottles were incubated in the dark at 4°C for 2 h. At the end of the incubation, 0.5 ml of formalin was injected into the bottles to stop microbial activity and to preserve the sample. Samples were subsequently frozen and transported to Menlo Park, California, for analysis. Nitrous oxide was determined on a gas chromatograph (Shimadzu Scientific Instruments) equipped with a 63-Ni electron capture detector, as described by Duff et al. (1996).

Table 1. Summary of the two Green Creek tracer experiments.

	1995	1999
Q (L s^{-1})	3.0–0.3	23.0–28.0
Reach length (m)	497	357
Time of injection (h)	2.17	5.0
Width of wetted channel (m)	0.5–1.0	3.0–4.0

Stream tracer experiments—Two whole-stream nutrient enrichment tracer injections were conducted, the first on 13 January 1995, and the second on 06 January 1999. The 1995 experimental protocol is discussed by McKnight et al. (2004), and a summary is presented in Table 1. Stream discharge was measured at the Green Creek gauge site (F9, 5 m downstream of Transect #3) in the 1999 experiment (Fig. 2) at 15-min intervals. The flow rates and width of the wetted channel differed between the two experiments (Table 1). During the 1995 experiment, stream flow was low and decreased over time from 3 L s^{-1} to 0.3 L s^{-1}. The active channel width was 0.5 to 1.0 m. During the 1999 experiment, stream flow was generally steady at 23 L s^{-1}. However, 10 h prior to the experiment the stream flow had been much higher at 80 L s^{-1} (Fig. 3). Flow increased gradually

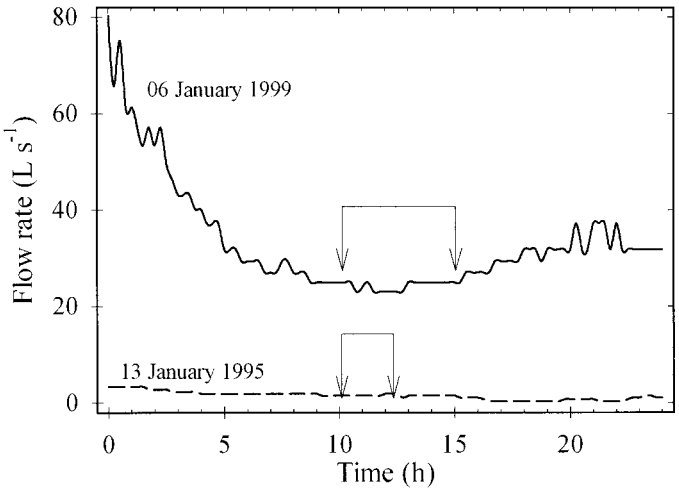

Fig. 3. Hydrographs for Green Creek for 13 January 1995 and 06 January 1999, beginning 10 h before start of the experiment. Arrows denote the beginning and end of the injection.

throughout the afternoon (Fig. 3). The width of the wetted channel was 3–4 m. In January 1999, an injection station was established near the outlet of a pond at the base of the Canada Glacier, and four sample sites were established downstream at varying distances (Fig. 1). Both experiments employed injection solutions that consisted of $NaNO_3$, K_2HPO_4, and LiCl dissolved in stream water. The 1999 injection rate was 35 ml min^{-1} for 2.5 h (beginning at 1200 h) and then increased to 50 ml min^{-1} for another 2.5 h (ending at 1700 h) as a result of battery failure and replacement. The total sampling time was 8 h, including the 5-h injection. Surface-water and sediment pore-water samples were collected at each site; surface samples were also collected immediately upstream of the injection point. Subsurface water was obtained from a 5.1-cm–diameter polyvinylchloride well emplaced 15 cm under the thalweg of the stream. The stream and well were sampled at 20-min intervals before, during, and after the injection.

Stream samples were collected as a single grab after three rinses. Well-water samples were extracted with a Nalgene hand pump. All samples were immediately filtered on site with GeoPumps and 0.4-μm GeoFilters (Geotech Environmental Equipment) and were frozen. Duplicate 125-ml samples were collected from both the stream and the well at each site. One sample was analyzed for NO_3^- on a Lachat Quickchem autoanalyzer (Lachat Instruments), with detection limits of 0.7 μmol N L^{-1}, at the Crary Lab in McMurdo, Antarctica, using standard methods. The sample was refrozen immediately after analysis. This sample was subsequently analyzed for NO_2^- in Boulder, Colorado, on a Lachat QuikChem 8000 Spectophotometric Flow Injection Analyzer using standard methods with a detection limit of 0.09 μmol N L^{-1}. The second set was brought back to Boulder for Cl^- analysis using a Dionex model 2022 ion chromatograph.

Transient storage modeling—The standard single transient storage zone model (SSZM) was used, as coded in the one-dimensional solute transport (OTIS) model (Runkel 1998), to test the hypothesis of McKnight et al. (2004) that denitrification was occurring in the hyporheic zone sediments, producing the observed stream NO_2^- concentrations. We also used a two-storage zone model (TSZM), as developed by Choi et al. (2000), to simulate stream solute transport to test the hypothesis that two unique storage zones corresponding to (1) microbial mats and (2) the hyporheic zone existed and influenced biogeochemical cycling of NO_3^-. The TSZM allowed for the representation of the system presented in Fig. 2, defined by

$$\frac{\partial C}{\partial t} = -\frac{Q}{A}\frac{\partial C}{\partial x} + \frac{1}{A}\frac{\partial}{\partial x}\left(AD\frac{\partial C}{\partial x}\right) + \frac{q_L}{A}(C_L - C) + \alpha_{MAT}(C_{MAT} - C) + \alpha_{HYP}(C_{HYP} - C) \quad (1)$$

$$\frac{\partial C_{MAT}}{\partial t} = \alpha_{MAT}\frac{A}{A_{MAT}}(C - C_{MAT}) - \lambda_{MAT}C_{MAT} \quad (2)$$

$$\frac{\partial C_{HYP}}{\partial t} = \alpha_{HYP}\frac{A}{A_{HYP}}(C - C_{HYP}) - \lambda_{HYP}C_{HYP} \quad (3)$$

where x is the distance downstream; t is time (s); D is the dispersion coefficient (m^2 s^{-1}); Q is the flow rate in the main channel (m^3 s^{-1}); C, C_{MAT}, and C_{HYP} represent the solute concentrations in the stream channel (μmol L^{-1}), the microbial mat, and the hyporheic zone, respectively; A, A_{MAT}, and A_{HYP} represent the cross-sectional area of the main channel, the microbial mat, and the hyporheic zone (m^2); α_{MAT} and α_{HYP} represent the exchange coefficients between the main channel and the microbial mat, and the main channel and the hyporheic zone (s^{-1}), respectively; λ_{MAT}, and λ_{HYP} represent the first-order removal coefficients in the microbial mat and hyporheic zone (s^{-1}), respectively; q_L is the lateral inflow rate per meter of stream length (m^3 s^{-1} m^{-1}; equivalent to m^2 s^{-1}); and C_L is the concentration of lateral inflows (μmol L^{-1}). Because dissimilatory NO_3^- reduction to NO_2^- requires anoxic zones, this process is much more likely to occur in the microbial mat and hyporheic zone than in the water column. Transformation of NO_3^- to NO_2^- was represented as a proportion of the first order NO_3^- removal in both the microbial mat,

$$\frac{\partial C_{MAT,NO_2}}{\partial t} = \alpha_{MAT}\frac{A}{A_{MAT}}(C_{NO_2} - C_{MAT,NO_2}) + \gamma_{NO_2}\lambda_{MAT}C_{MAT,NO_3} \quad (4)$$

and in the hyporheic zone

$$\frac{\partial C_{HYP,NO_2}}{\partial t} = \alpha_{HYP}\frac{A}{A_{HYP}}(C_{NO_2} - C_{HYP,NO_2}) + \gamma_{NO_2}\lambda_{HYP}C_{HYP,NO_3} \quad (5)$$

This formulation allows for independent rate constants to be estimated for NO_3^- removal in the microbial mat (λ_{MAT}), and the hyporheic zone (λ_{HYP}), and for NO_2^- production (γ_{NO_2}). Because the NO_2^- production parameter (γ) is expressed as a proportion of NO_3^- uptake rate (λ), it is unitless; it represents the proportion of NO_3^- removed that is converted to NO_2^- and not further reduced. All transport simulations were made by modifying the transient storage model as described above, within the OTIS software package (Runkel 1998).

Single storage zone model fits for the conservative transport of Cl^- and first-order removal of NO_3^- from the 1995 experiment reported by McKnight et al. (2004) were not changed. Model parameter regressions based on the conservative hydrologic tracer (Cl^-) for the SSZM were accomplished with UCODE (Poeter and Hill 1998), a universal inverse model software package, as described by Scott et al. (2003). Transient storage simulations of the 1995 and 1999 data sets were run in a particular sequence, first simulating conservative Cl^- transport, then NO_3^- transport and removal in the stream and in the hyporheic zone, and finally NO_2^- production in the stream and in the hyporheic zone, with the SSZM. Further simulations with the TSZM (Eqs. 1–5) were run again in the same sequence, Cl^-, then for NO_3^- transport and removal, and finally for NO_2^- production, also optimized with UCODE. The parameters A and D were held fixed from the SSZM simulations.

In order to simulate the conservative transport of Cl^- properly in both SSZM and TSZM for the 1999 data set, lateral inflows of 0.0, 3.01×10^{-5}, 8.99×10^{-5}, and 3.84×10^{-5} m^3 s^{-1} m^{-1} were required for each downstream reach,

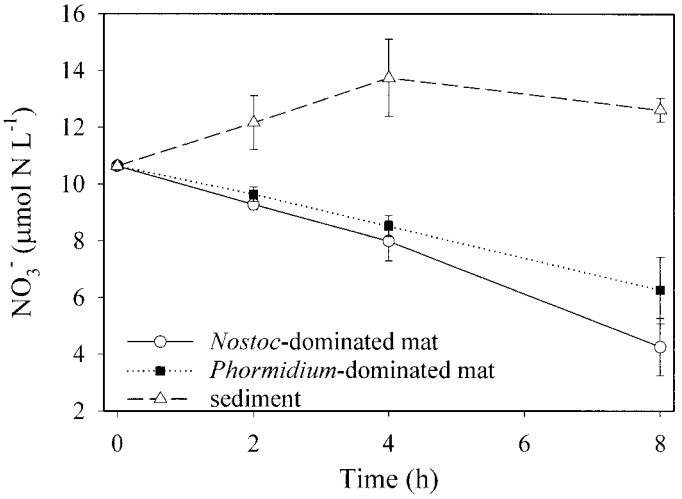

Fig. 4. NO_3^- uptake rates observed in mesocosm incubations of *Phormidium* spp.–dominated orange microbial mat, *Nostoc* spp.–dominated black microbial mat, and sediment samples from Green Creek, Antarctica. Bars represent standard deviations of three replicates.

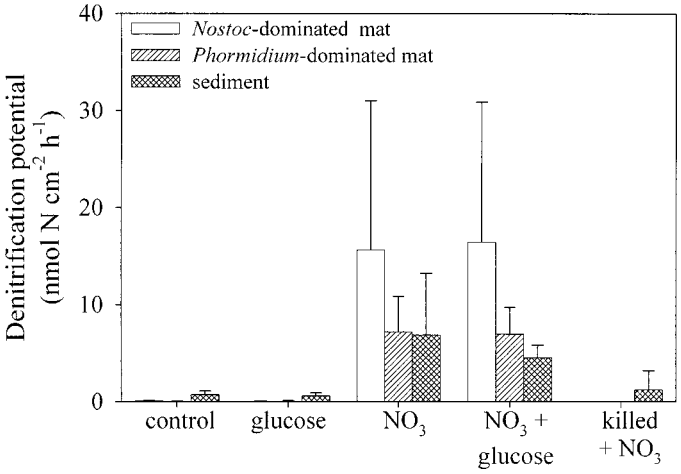

Fig. 5. Denitrification potential rates observed in mesocosm incubations of *Nostoc* spp. (black) microbial mat, *Phormidium* spp. (orange) microbial mat, and sediment samples from Green Creek, Antarctica. Bars represent standard deviations of three replicates.

respectively. C_L values were set to 2.4 μmol L^{-1} for Cl^-, 17.0 μmol L^{-1} for NO_3^-, and 0.0 μmol L^{-1} for NO_2^-, similar to concentrations of hyporheic water found by Gooseff (unpubl. data) and reported by Gooseff et al. (2003). These lateral inflows most likely correspond to bank storage returning to the stream after much higher discharges the previous night (Fig. 3).

The TSZM was parameterized using α_{MAT} values from previous studies of periphyton nutrient uptake in flumes, so that α_{HYP}, A_{HYP}, and A_{MAT} were optimized in conservative TSZM simulations. Mulholland et al. (1994) conducted a series of flume experiments using natural stream water to study the effect of an established periphyton community on solute transport. Their results showed that the effective storage zone created by the periphyton was characterized by an equation in which A_S divided by A yields roughly 0.18 (where A_S represents the cross-sectional area of the storage zone in the system of study, here we differentiate between A_{MAT} and A_{HYP}) and an exchange coefficient (α) of 4.4 × 10^{-2} s^{-1}. Similarly, Kim et al. (1990) studied periphyton effects on N transport in a small flume structure that was placed in Little Lost Man Creek, California. Their results also showed that the effective storage zone created by the periphyton was characterized by an A_S/A value of roughly 0.17, but their results yielded an exchange coefficient almost an order of magnitude lower, 5.25 × 10^{-3} s^{-1}. In order to constrain the TSZM simulations presented here, we used both of these previously determined α values to represent exchange with the microbial mat, α_{MAT}. Model runs using each α_{MAT} value are referred to as ''Mul'' and ''Kim,'' respectively. A_{MAT} was assigned the same value for each reach, determined by trial and error, such that the Cl^- stream solute concentrations were not substantially changed in simulations with the TSZM, compared to SSZM simulations. TSZM NO_3^- hyporheic removal rates (λ_{HYP}) were assumed to be the same as rates obtained in single storage zone modeling. TSZM λ_{MAT} rates were estimated using UCODE. Stream NO_3^- breakthrough curves were not changed substantially from single storage zone NO_3^- transport modeling.

Calculating ambient NO_3^- uptake—Because of the sensitive nature of the closed-basin dry valley aquatic ecosystems, our experimental design did not include stable isotopes as nutrient tracers. Dodds et al. (2002) have argued that uptake parameters from nutrient addition experiments scale with the level of nutrient enrichment. In order to calculate an ambient NO_3^- uptake rate, we use the plateau NO_3^- concentrations from our two whole-stream experiments to calculate uptake flux (U_t) of NO_3^- and to develop a relationship between nutrient concentration (C_n) and U_t, as outlined by Dodds et al. (2002). We then regress a natural U_t corresponding to the background C_n values.

Results

Mesocosm experiments—The highest NO_3^- uptake rates were observed in the first 2 h: 16.2 nmol N cm^{-2} h^{-1} for *Nostoc* spp.–dominated microbial mats and 11.9 nmol N cm^{-2} h^{-1} for predominantly *Phormidium* spp. microbial mats (Fig. 4). In the sediment assays, NO_3^- was released. Over 8 h, NO_3^- was released at an effective rate of 7 nmol N cm^{-2} h^{-1}. The denitrification assays showed that NO_3^-, but not glucose, stimulated denitrifying activity in sediment and microbial mats (Fig. 5), indicating that for these incubation conditions, sufficient electron donor was present to support denitrification. Denitrifying activity was greater in the *Nostoc* spp. mats than in either the *Phormidium* spp. mats or the sediments (Fig. 5). Denitrification potentials ranged from 4.5 nmol N cm^{-2} h^{-1} in the sediment to 16.4 nmol N cm^{-2} h^{-1} in predominantly *Nostoc* spp. microbial mats. Relatively little activity was observed in any assays without adding NO_3^- or when assays were killed with formalin. The measurable denitrification potential in the killed sediment mesocosms indicates that our kill procedure may not have been com-

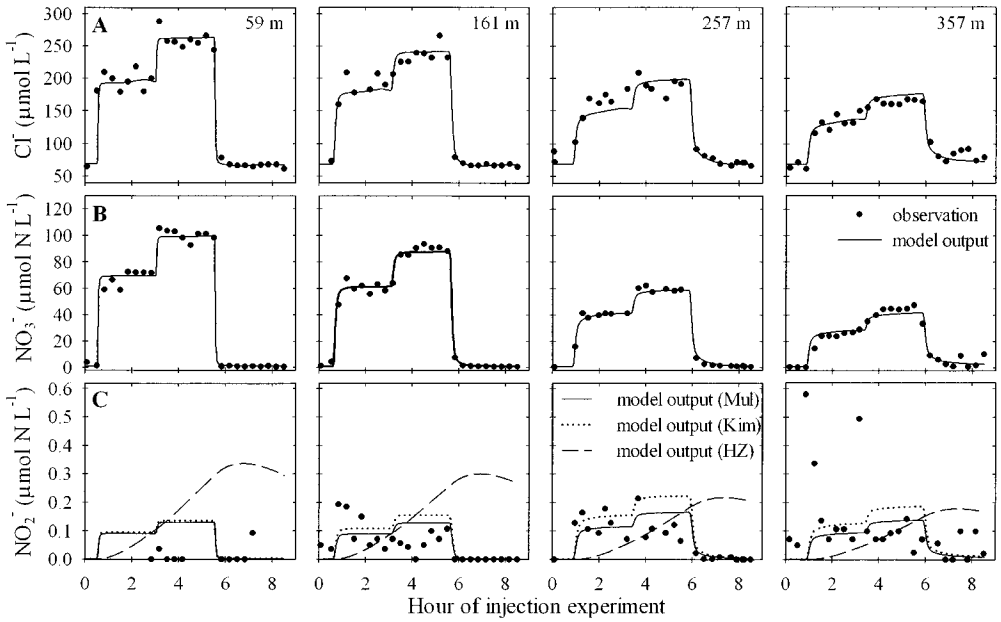

Fig. 6. Stream observations (points) and model fit (line) from the 1999 Green Creek tracer injection experiment, for concentrations of (A) Cl^- (conservative tracer), (B) NO_3^-, and (C) NO_2^-. Model fits for stream NO_2^- are presented for TSZM simulations using α_{MAT} values from Mulholland et al. (1994), ''Mul,'' α_{MAT} values from Kim et al. (1990), ''Kim,'' and SSZM NO_2^- production in the hyporheic zone only assuming 100% conversion of NO_3^- taken up, ''HZ.''

pletely effective on sediment biota. *Nostoc* spp. mat denitrification potential was comparable to *Nostoc* spp. mat NO_3^- uptake rate, and predominantly *Phormidium* spp. mat denitrification potential was less than half of the *Phormidium* spp. mat NO_3^- uptake rate.

Whole-stream tracer experiment and transient storage modeling—The results of the 1999 stream tracer experiment are presented in Fig. 6. Solute transport simulations of Cl^- and NO_3^- using the TSZM closely match the observed data (Fig. 6A,B). The Cl^- and NO_3^- concentrations increased during plateau because the injection rate changed. The plateau concentrations decreased downstream due to lateral inflow from bank storage.

The eight stream samples collected upstream of the injection point during the 1999 experiment had NO_2^- concentrations lower than the detection limit. A sample of the injection solution analyzed for NO_2^- was also found to be below detection limits. Below the injection site, changes in stream NO_2^- concentrations, though small, generally coincided with changes in NO_3^-, increasing downstream while NO_3^- concentrations decreased (Fig. 6B,C). Stream NO_2^- concentrations resulted from N cycling processes during downstream transport. TSZM NO_2^- simulations show the NO_2^- concentrations increasing in the stream in the same time period as the observed data, with concentrations generally in the same range as the data (Fig. 6C).

SSZM NO_2^- simulations (assuming that 100% of the NO_3^- that is biotically removed from the stream between each station was converted to NO_2^- by dissimilatory processes in the hyporheic zone) predicted NO_2^- pulses would occur significantly later than was observed at each station (Fig. 6C; dashed line). This time lag between observed and simulated NO_2^- pulses is the result of hyporheic exchange and represents a transport limitation. The notion that incomplete denitrification is occurring only in the hyporheic zone does not conform to the observed timing of the NO_2^- pulses; instead the NO_2^- must be produced in a benthic zone with faster exchange with stream water.

Chloride and NO_3^- concentrations collected from the in-stream wells are presented in Fig. 7A and B. The simulated concentrations for hyporheic concentrations agreed closely with the observed data for Cl^- and NO_3^- at sites 1, 3, and 4, but not for site 2. NO_2^- concentrations collected from the in-stream wells were similar in magnitude to stream observations and significantly lower than NO_3^- concentrations. The simulated concentrations for hyporheic NO_2^- are shown in Fig. 7C. It is important to note that only stream solute (Cl^-, NO_3^-, NO_2^-) data were used in the optimization of transient storage and biogeochemical model parameters.

For all 1999 TSZM simulations, optimized A values for SSZM Cl^- transport were used, ranging from 0.002 to 0.33 m^2, and A_{MAT} was determined to be 0.01 m^2, using the α_{MAT} values from Mulholland et al. (1994) and Kim et al. (1990) (Table 2). This A_{MAT} value is small but reasonable, considering that benthic microbial mats are 0.001–0.02 m thick (Vincent et al. 1993*a*) and that 3–4 m of stream width may be covered by microbial mats. At the higher flow in the 1999 experiment, the entire 3–4 m of stream width covered by microbial mats were also covered by stream flow. Optimal A_{HYP} values ranged from 0.02 to 1.05 m^2, and α_{HYP} values ranged from 1.16×10^{-4} to 3.16×10^{-2} s^{-1}.

Chloride, NO_3^-, and NO_2^- simulations from the 1995 stream tracer experiment are presented in Fig. 8. The Cl^- and NO_3^- simulations were reported by McKnight et al. (2004). A NO_2^- pulse occurred at the three upstream sta-

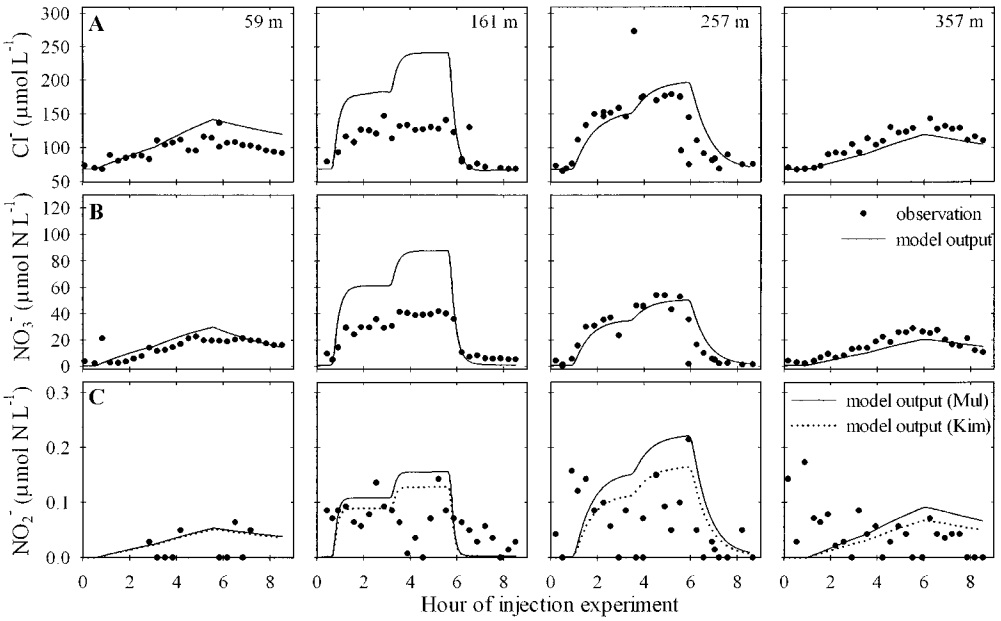

Fig. 7. Hyporheic (in-stream well) observations (points) and model fit (line) from 1999 Green Creek tracer injection experiment for concentrations of (A) Cl^-, (B) NO_3^-, and (C) NO_2^-. Model fits for stream NO_2^- are presented for TSZM simulations using α_{MAT} values from Mulholland et al. (1994), ''Mul,'' α_{MAT} values from Kim et al. (1990), ''Kim,'' and SSZM NO_2^- production in the hyporheic zone only assuming 100% conversion of NO_3^- taken up, ''HZ.''

tions, coincident with NO_3^-, but at much lower concentrations, below 0.6 μmol N L^{-1} (Fig. 8C). The NO_2^- pulse was well defined and had a shorter duration than the NO_3^- pulse. The detection limit for the NO_2^- analyses in this data set was 0.15 μmol N L^{-1}; therefore, the tail of the stream NO_2^- pulse may have been at or below the detection limit, resulting in the reduced temporal resolution of the NO_2^- pulse compared to the 1999 results (Fig. 6C).

Optimized parameter estimates for the 1995 simulations are reported in Table 3. Relative sum of squared residual (SOSR) values were minimized for each scenario. A_{MAT} values were 0.001 m^2 for all reaches; these values were small enough that there was no substantial change to the simulated stream solute concentrations. This cross-sectional area was an order of magnitude lower than A_{MAT} found in the 1999 simulations, but this is reasonable given that microbial mats may be 0.001–0.02 m thick (Vincent et al. 1993*a*) and cover 0.5 to 1.0 m of the active stream width at very low flow. The very low flow ($<$3.0 L s^{-1}) during the 1995 tracer experiment resulted in small A values (ranging from 2 to 7 $\times$ 10^{-2} m^2). Calculated A_{MAT}:A ratios ranged from 0.01 to 0.05.

The NO_2^- conversion parameter (γ) represents the ratio of the NO_2^- production rate to the NO_3^- removal rate in the microbial mat, which is assumed to be the proportion of

Table 2. Parameter values from the best-fit simulations for the 1999 Green Creek tracer experiment. Conservative transport parameter values were used in reactive transport modeling. Two-storage zone model (TSZM) simulation parameter values for Mulholland et al. (1994), ''Mul,'' and Kim et al. (1990), ''Kim,'' are differentiated where noted. Note: A_{MAT} was 0.01 m^2, and α_{MAT} was 4.40 $\times$ 10^{-2} and 5.25 $\times$ 10^{-3} (Mul and Kim, repsectively).

Reach No.	A (m^2)	A_{HYP} (m^2)	α_{HYP} (s^{-1})	Transient storage model parameter: λ (s^{-1})	λ_{HYP} (s^{-1})	λ_{MAT} (s^{-1}) Mul	γ (s^{-1}) Mul	λ_{MAT} (s^{-1}) Kim	γ (s^{-1}) Kim
	SSZM, conservative transport			SSZM, reactive transport					
1	0.09	0.304	1.16×10^{-4}	5.32×10^{-4}	3.72×10^{-5}	—	—	—	—
2	0.13	0.020	2.07×10^{-4}	1.90×10^{-5}	0	—	—	—	—
3	0.33	0.132	1.75×10^{-4}	9.86×10^{-5}	6.81×10^{-5}	—	—	—	—
4	0.002	1.050	3.16×10^{-2}	3.87×10^{-2}	0	—	—	—	—
	TSZM, conservative transport			TSZM, reactive transport (Mul, Kim)					
1	0.09	0.294	1.16×10^{-4}	—	3.72×10^{-5}	4.62×10^{-3}	0.034	4.99×10^{-3}	0.200
2	0.13	0.010	2.07×10^{-4}	—	0	1.69×10^{-4}	0.139	2.06×10^{-4}	0.202
3	0.33	0.122	1.75×10^{-4}	—	6.81×10^{-5}	2.13×10^{-3}	0.037	4.64×10^{-3}	0.042
4	0.002	1.040	3.16×10^{-2}	—	0	1.98×10^{-1}	0.0	1.0	0.0

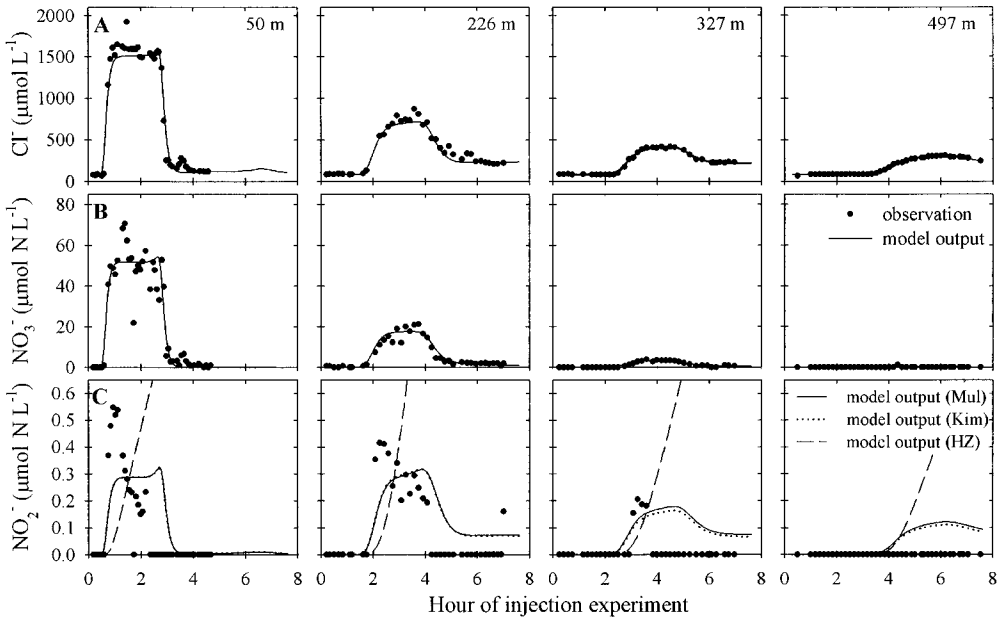

Fig. 8. Stream observations (points) and model fit (line) from the 1995 Green Creek tracer injection experiment for concentrations of (A) Cl^- (conservative tracer), (B) NO_3^-, and (C) NO_2^-. Model fits for stream NO_2^- are presented for TSZM simulations using α_{MAT} values from Mulholland et al. (1994), ''Mul,'' α_{MAT} values from Kim et al. (1990), ''Kim,'' and SSZM NO_2^- production in the hyporheic zone only assuming 100% conversion of NO_3^- taken up, ''HZ.''

NO_3^- reduced to NO_2^- by dissimilatory microbial processes. The proportion of NO_3^- assimilated by microbial mats or completely denitrified by bacteria is calculated as $(1 - \gamma)$. For the 1995 tracer experiment, model runs based on the alternative α_{MAT} exchange rates estimated by Kim et al. (1990) and Mulholland et al. (1994) indicated that 2.1%, 5.0%, 0%, and 0%, and 1.5%, 3.4%, 0%, and 0%, respectively, of NO_3^- removed by microbial mats and hyporheic zone was converted to NO_2^- by the associated microbial community between each sampling station (Table 3). For the 1999 tracer experiment, using the α_{MAT} exchange value from Kim et al. (1990) and Mulholland et al. (1994), 20.0%, 20.2%, 4.2%, and 0%, and 3.4%, 13.9%, 3.7%, and 0%, respectively, of NO_3^- removed by the microbial mats and hyporheic zone was converted to NO_2^- (Table 2).

NO_3^- uptake rate—Using the plateau NO_3^- concentrations from the 1995 and 1999 injection experiments, we computed uptake lengths of 113.6 m and 344.8 m, respectively. NO_3^- uptake rates are computed to be 0.66 μmol N m^{-2} s^{-1} for the 1995 experiment, given a NO_3^- concentration of 50.0 μmol N L^{-1}, and 1.90 μmol m^{-2} s^{-1} for the 1999 experiment, given a NO_3^- concentration of 100 μmol N L^{-1} (Fig. 9). Assuming that zero NO_3^- corresponds to no uptake,

Table 3. Parameter values from the best-fit simulations for the 1995 Green Creek tracer experiment. Conservative transport parameter values were used in reactive transport modeling. TSZM simulation parameter values for Mulholland et al. (1994), ''Mul,'' and Kim et al. (1990), ''Kim,'' are differentiated where noted. Note: A_{MAT} was 0.001 m^2, and α_{MAT} was 4.40×10^{-2} and 5.25×10^{-3} (Mul and Kim, respectively).

Reach No.	A (m^2)	A_{HYP} (m^2)	α_{HYP} (s^{-1})	Transient storage model parameter: λ (s^{-1})	λ_{HYP} (s^{-1})	λ_{MAT} (s^{-1}) Mul	γ (s^{-1}) Mul	λ_{MAT} (s^{-1}) Kim	γ (s^{-1}) Kim
	SSZM, conservative transport			SSZM, reactive transport					
1	0.02–0.07	0.045	3.46×10^{-5}	2.3×10^{-4}	1.8×10^{-5}	—	—	—	—
2	0.02–0.07	0.400	1.89×10^{-4}	4.3×10^{-5}	1.1×10^{-4}	—	—	—	—
3	0.02–0.07	0.39	2.72×10^{-4}	3.9×10^{-5}	3.3×10^{-6}	—	—	—	—
4	0.02–0.07	0.070	1.14×10^{-2}	0.0	0.0	—	—	—	—
	TSZM, conservative transport			TSZM, reactive transport (Mul, Kim)					
1	0.02–0.07	0.044	3.46×10^{-5}	—	1.8×10^{-5}	1.58×10^{-2}	0.015	1.63×10^{-2}	0.021
2	0.02–0.07	0.399	1.89×10^{-4}	—	1.1×10^{-4}	3.77×10^{-3}	0.034	3.41×10^{-3}	0.050
3	0.02–0.07	0.389	2.72×10^{-4}	—	3.3×10^{-6}	1.43×10^{-2}	0.000	2.28×10^{-2}	0.000
4	0.02–0.07	0.069	1.14×10^{-2}	—	0.0	1.0	0.000	4.17×10^{-2}	0.000

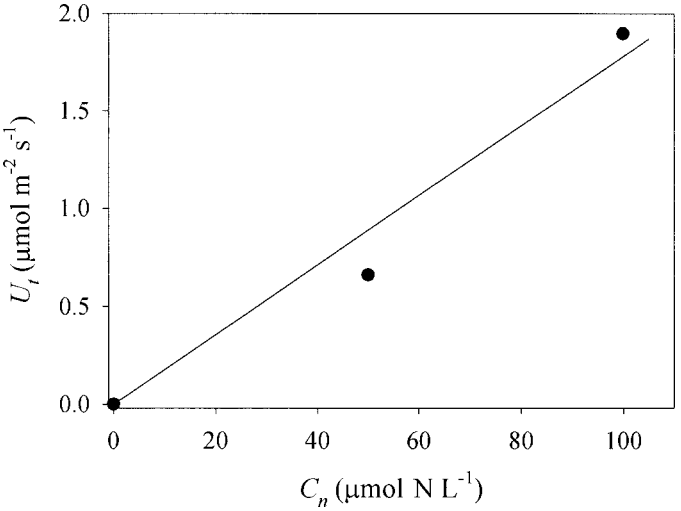

Fig. 9. Nitrate uptake rate (U_t) as a function of concentration, showing the regression relationship based on the 1995 and 1999 Green Creek tracer injection experiments, with the line forced through zero.

the regression equation relating uptake rate to nutrient concentration is $U_t = 0.0178C_n$ ($r^2 = 0.91$). Thus, at ambient NO_3^- concentration of 0.25 μmol N L^{-1} (McKnight et al. 2004), the uptake rate is approximately 0.004 μmol N m^{-2} s^{-1}.

Discussion

Evidence of NO_3^- uptake from assay experiments—Both the N-uptake and denitrification mesocosm assays indicated that benthic microbial mats were the primary location of NO_3^- removal in Green Creek (Figs. 4, 5). The results indicate that NO_3^- uptake associated with photosynthesis in predominantly *Nostoc* and *Phormidium* spp. microbial mats is a primary mechanism for NO_3^- removal in glacial meltwater streams. In addition, the microbiota associated with the microbial mats had greater denitrification potentials than sediment microbiota and were more likely to reduce NO_3^- through denitrification than were microbiota in sediments. Potential denitrification rates calculated from denitrification assays were comparable to NO_3^- uptake rates associated with *Nostoc* spp. and *Phormidium* spp. algae. Microbial mats form an habitat in which denitrification may be expected because of available decomposing carbohydrates, often-steep oxygen gradients (Vincent et al. 1993*a*), and occasionally high nitrate concentrations.

Denitrification potentials were NO_3^--limited rather than C-limited in the assays (Fig. 5). These results are surprising, considering the low dissolved organic carbon (DOC) concentrations of dry valley streams (generally less than 50 μmol C L^{-1}), and indicate that microbially derived DOC input to meltwater streams is labile and that its respiration by denitrifying bacteria is limited by oxidant availability.

During the NO_3^- uptake experiments, sediments released NO_3^- into the overlying water (Fig. 4). This release was probably associated with NH_4^+ desorption from sediments. Potassium, introduced into the incubations as KNO_3, may have competed with NH_4^+ for mineral binding sites, causing its release and subsequent nitrification to NO_3^-. This is plausible because anaerobic microsites are likely diminished when sediments are removed from the stream and because apparently oxygenated sediments can have some potential denitrification activity (Dodds and Jones 1987). If nitrification is a potential source of NO_3^- in the assay experiments, it is possibly also a source of NO_2^- in the stream. We cannot rule out nitrification as a source of stream NO_2^-, but the coincidence of observed NO_3^- uptake and NO_2^- production indicates a more likely link between denitrification activity and NO_3^- losses, resulting in NO_2^- production in a single reduction step, rather than an ion exchange reaction and subsequent nitrification of liberated NH_4^+. Further evidence comes from a separate analysis of injected K^+ dynamics during the 1995 Green Creek experiment, in which Gooseff et al. (in press) found that the streambed was not a consistent sink of K^+. Thus, the streambed is likely not a consistent source of NH_4^+, suggesting that nitrification is a less likely source of NO_2^-.

Reach-scale NO_3^- uptake—Our findings are similar to those of Dodds et al. (2002), in whose study increased nutrient concentration apparently stimulated increased nutrient uptake. The computed ambient NO_3^- uptake flux for Green Creek is lower than those reported by Dodds et al. (2002) for temperate streams, because of a low ambient NO_3^- concentration. As McKnight et al. (2004) point out, the ambient NO_3^- concentrations are low because of the presence of extensive microbial mats. The method put forth by Dodds et al. (2002) does not explicitly account for differential losses of stream NO_3^- in distinct transient storage locations, whereas with the TSZM, we can assess differences between uptake coefficients in microbial mats and in the hyporheic zone. The TSZM results show that the microbial mat uptake coefficients were higher in the 1995 experiment than in the 1999 experiment (Tables 2, 3), but hyporheic uptake coefficients were greater in two reaches in the 1999 experiment than in the 1995 experiment. Because the reaches in both whole-stream experiments do not exactly overlap (the 1995 experiment was over a longer reach), the comparison is not ideal.

Reach-scale denitrification and the two-storage zone model—Denitrifying activity was evident in the reach-scale NO_3^- transport simulations as well as in mesocosm experiments, indicating that anoxic microzones support an active denitrifying population of microbes. These potentials are consistent with the results of Kemp and Dodds (2001), who found very steep DO gradients over very short spatial scales in temperate stream sediments, resulting in environments conducive to denitrification.

Nitrite simulations quantitatively show that most of the NO_3^- taken up was assimilated or completely denitrified and that dissimilatory reduction to NO_2^- was minor. Nitrate removal in Green Creek by biotic assimilation and denitrification can be separated from dissimilatory reduction to NO_2^- using the whole-stream tracer simulations, assuming that NO_3^- disappearance in excess of the NO_2^- formed is due either to denitrification or assimilation by algae and microorganisms (in either storage zone), or a combination of both.

Unlike the results from a temperate stream in southern Canada (Hill 1979), the simulations presented here indicate that the majority of NO_3^- lost from Green Creek was either assimilated or denitrified (up to 100% for some reaches) and that only a smaller proportion was reduced to NO_2^- (no more than 21%). Together, results from mesocosm and reach-scale experiments indicate that NO_3^- reduction to NO_2^- is a relatively small percentage of NO_3^- removal in Green Creek.

Dissimilatory NO_3^- reduction is rapid and has to be occurring in the microbial mats, which exchange water more rapidly with the water column, not just in the hyporheic zone, where exchange is slower. The relative timing of the NO_2^- pulses at each station compared with the NO_3^- removal indicates that dissimilatory NO_3^- reduction to NO_2^- occurs rapidly (on the time scale of stream advection). Data from the denitrification assays and observations of elevated NO_2^- levels in hyporheic wells indicate that denitrification, with NO_2^- accumulating transiently, occurred in the hyporheic zone. Reactive transport simulations with the SSZM, however, showed that the hyporheic compartment alone could not explain the observed stream NO_2^- data (Figs. 6C, 8C). Exchange coefficients for the hyporheic zone (mostly on the order of 10^{-4} s^{-1} for these reaches) were too slow to transport hyporheic-generated NO_2^- into the stream as fast as stream-water NO_2^- accumulated during the tracer experiment. Moreover, previous findings by Vincent et al. (1993*a*) of a deep chlorophyll *a* maximum and steep DO gradients within dry valley benthic microbial mats imply that microbial mats are the most likely location of NO_2^- formation in the two whole-stream NO_3^- enrichment experiments. These observations provide evidence that the TSZM is appropriate to simulate NO_3^- transport and fate in dry valley streams.

The complexity of N cycling within the microbial mats may influence the detailed pattern of NO_2^- observations. Nitrite concentrations observed early in the pulse may indicate rapid microbial response to the large pulse of NO_3^-. In the context of the glacial meltwater environment, it is reasonable to assume that the microbes that survive are those that can take advantage of nutrients quickly when they are present. By the same token, the early NO_2^- concentrations (at the beginning of the NO_2^- pulse) may be the result of the sequential induction of NO_3^- reductase before NO_2^- reductase. The NO_2^- simulations are constrained by the first-order conversion approach we have used to model NO_3^- reduction to NO_2^-, and the simulated NO_2^- pulses have the same shape as the NO_3^- pulse because of the direct dependence on NO_3^- concentrations in the microbial mat.

Choi et al. (2000) showed that multiple storage zone models were useful when multiple time scales of exchange could be clearly identified. In this study, we used biogeochemical evidence consisting of NO_2^- formation from dissimilatory NO_3^- reduction, conservative Cl^- transport, and our understanding of denitrification reactions in dry valley stream microbial communities to justify the use of the TSZM. The TSZM stream NO_2^- simulations, while imperfect, generally captured the timing and magnitude of the observations from both experiments.

At the reach scale, using the TSZM, A_{MAT} values were generally an order of magnitude smaller than the A_{HYP} values for the 1995 and 1999 tracer experiment simulations. In both years, A_{MAT} values were specified to be small enough so that the areas did not store too much solute, and as a result, the stream solute simulations were not drastically changed during calibration model runs. In the 1995 simulations, the high α_{HYP} value and small A_{HYP}, derived from the SSZM simulations for reach 4, limited the effectiveness of modeling the microbial mat storage zone using the Kim et al. (1990) α_{MAT} value. Essentially, the storage zones were competing because the solute flux to each zone was similar in magnitude. If A_{MAT} were much larger, the balance between hyporheic zone and stream channel that was established with the single storage zone model would be disrupted. At very low flow, the microbial mats are in contact with a substantial portion of the water column at all times. Physically, one interpretation of the A_{MAT} value is that it represents the proportion of the total cross-sectional area of the microbial mat that is effectively exchanging on the time scale associated with α_{MAT}.

NO_3^- uptake rates in the microbial mat are one to two orders of magnitude higher than the stream NO_3^- uptake rates found for the single hyporheic zone model (Tables 2, 3). The difference is the transport lag between the stream and the microbial mat, which is on the order of 10^{-3} to 10^{-2} s^{-1}. NO_3^- uptake rates in the microbial mat must be higher than those for the stream (in the single storage zone model) because of the time scale of hydrologic transport into and out of the microbial mat. As a consequence, microbial mat residence times are very short, on the order of seconds.

The TSZM was useful for computing reach-scale NO_3^- uptake rates for biotically active benthic components. Because the reduction of NO_3^- to NO_2^- takes place on the time scale of stream-water transport, the dissimilatory reduction could have been simulated to occur in the water column in the same way that NO_3^- uptake by the microbial mats was represented as occurring in the water column by McKnight et al. (2004). The TSZM provides a more accurate representation of the process, though, because NO_3^- reduction is not likely to occur in the oxic, oligotrophic conditions of the water column. Our results show that incorporating the results from laboratory studies of hyporheic exchange for microbial mats/periphyton yields satisfactory results in reach-scale simulations of solute transport.

The TSZM defines and simulates two distinct and independent storage zones, whereas the hydrologic storage within a coupled stream-hyporheic system is more likely a continuum beginning in the water column with little storage, moving out toward more distal subsurface locations with longer storage. Surface bed sediments are likely exchanging rapidly with the stream and very slowly with the deep or further sediments (e.g., lateral locations) (Gooseff et al. 2003). Further, the microbial layer extends the faster exchange layer into the water column, but even within the microbial mat, there is likely a gradient of exchange. The TSZM is only a first step toward the development of a more appropriate gradient-based exchange model.

Benthic microbial communities provide an important control on nutrient transport in dry valley streams. The results from microbial assays indicate that NO_3^- removal from stream water is due in large part to biotic assimilation rather than denitrification, which does not appear to be limited by carbon availability. It is possible that denitrification is lim-

ited by biotic NO_3^- assimilation, as both processes compete for available NO_3^-. Denitrification may also be limited by the rapid exchange of water between the stream and the benthic microbial mat. Nitrite may be carried by return flows into the stream before it can be converted to N_2O because of N_2O reductase limitation. Denitrification is likely a minor sink compared to biotic assimilation for stream NO_3^-, but is nonetheless important, as it is a source of NO_2^- and N_2O for other members of the microbial community. In the hyporheic zone, it is assumed that all NO_3^- loss is due to denitrification, some of which is incomplete.

In both tracer experiments, we observed a pulse of NO_2^- associated with the addition of NO_3^- to the stream. We interpret this biogeochemical signal to be evidence of a rapid hydrologic transient storage process, independent of slower hyporheic exchange, which is characterized by conservative solute tracer dynamics. The modeling approach taken in this study assumes that hydrologic exchange is happening on more than one time scale, is a rapid exchange between the stream and a storage zone created by the presence of microbial mats, and exhibits a longer time scale exchange between the stream and the hyporheic zone. The results show that the hydrologic exchange between the stream and benthic microbial mats has a direct effect on nutrient dynamics in dry valley streams.

References

ALGER, A. S., AND OTHERS. 1997. Ecological processes in a cold desert ecosystem: The abundance and species of algal mats in glacial meltwater streams in Taylor Valley, Antarctica. INSTAAR Occasional Paper no. 51.

BOMBLIES, A., D. M. MCNIGHT, AND E. D. ANDREWS. 2001. Retrospective simulation of lake-level rise in Lake Bonney based on recent 21-yr record: Indication of recent climate change in the McMurdo Dry Valleys, Antarctica. J. Paleolimnol. **25:** 477–492.

CHOI, J., J. W. HARVEY, AND M. H. CONKLIN. 2000. Use of multiparameter sensitivity analysis to determine relative importance of factors influencing natural attenuation of mining contaminants. Water Resource Res. **36:** 1511–1518.

DEANGELIS, D. L., M. LOREAU, D. NEERGAARD, P. J. MULHOLLAND, AND E. R. MARZOLF. 1995. Modelling nutrient–periphyton dynamics in streams: The importance of transient storage zones. Ecol. Model. **80:** 149–160.

DENT, C. L., AND J. C. HENRY. 1999. Modelling nutrient–periphyton dynamics in streams with surface–subsurface exchange. Ecol. Model. **122:** 97–116.

DODDS, W. K., AND B. J. BIGGS. 2002. Water velocity attenuation by stream periphyton and macrophytes in relation to growth form and architecture. J. N. Am. Benthol. Soc. **21:** 2–15.

———, AND R. D. JONES. 1987. Potential rates of nitrification and denitrification in an oligotrophic freshwater sediment system. Microb. Ecol. **14:** 91–100.

———, AND OTHERS. 2002. N uptake as a function of concentration in streams. J. N. Am. Benthol. Soc. **21:** 206–220.

DUFF, J. H., C. M. PRINGLE, AND F. J. TRISKA. 1996. Nitrate reduction in sediments of lowland tropical streams draining swamp forest in Costa Rica: An ecosystem perspective. Biogeochemistry **33:** 179–196.

———, AND F. J. TRISKA. 1990. Denitrification in sediments from the hyporheic zone adjacent to a small forested stream. Can. J. Fish. Aquat. Sci. **47:** 1140–1147.

GOOSEFF, M. N., D. M. MCKNIGHT, W. B. LYONS, AND A. E. BLUM. 2002. Weathering reactions and hyporheic exchange controls on stream water chemistry in a glacial meltwater stream in the McMurdo Dry Valleys. Water Resource Res. **38**: 1279.

———, ———, AND R. L. RUNKEL. In Press. Reach-scale cation exchange controls on major ion chemistry of an Antarctic glacial meltwater stream. Aquat. Geochem.

———, ———, ———, AND B. H. VAUGHN. 2003. Determining long timescale hydrologic flow paths in Antarctic streams. Hydrol. Proc. **17:** 1691–1710.

HILL, A. R. 1979. Denitrification in the nitrogen budget of a river ecosystem. Nature **281:** 291–293.

HOLMES, R. M., J. B. JONES, S. G. FISHER, AND N. B. GRIMM. 1996. Denitrification in a nitrogen-limited stream ecosystem. Biogeochemistry **33:** 125–146.

HOWARD-WILLIAMS, C., I. HAWES, A. M. SCHWARZ, AND J. A. HALL. 1997. Sources and sinks of nutrients in a polar desert stream, the Onyx River, Antarctica, p. 155–170. *In* W. B. Lyons and others [Eds.], Ecosystem processes in Antarctic ice-free landscapes. Balkema Press.

———, J. C. PRISCU, AND W. F. VINCENT. 1989. Nitrogen dynamics in two Antarctic streams. Hydrobiologia **172:** 51–61.

KEMP, M. J., AND W. K. DODDS. 2001. Centimeter-scale patterns in dissolved oxygen and nitrification rates in a prairie stream. J. N. Am. Benthol. Soc. **20:** 347–357.

KIM, B. K., A. P. JACKMAN, AND F. J. TRISKA. 1990. Modeling transient storage and nitrate uptake kinetics in a flume containing a natural periphyton community. Water Resource Res. **26:** 505–515.

———, ———, AND ———. 1992. Modeling biotic uptake by periphyton and transient hyporrheic storage of nitrate in a natural stream. Water Resource Res. **28:** 2743–2752.

KNOWLES, R. 1982. Denitrification. Microbiol. Rev. **46:** 43–61.

MARTIN, L. A., P. J. MULHOLLAND, J. R. WEBSTER, AND H. M. VALETT. 2001. Denitrification potential in sediments of headwater streams in the southern Appalachian Mountains, USA. J. N. Am. Benthol. Soc. **20:** 505–519.

MAURICE, P. A., D. M. MCKNIGHT, L. LEFF, J. E. FULGHUM, AND M. GOOSEFF. 2002. Direct observations of aluminosilicate weathering in the hyporheic zone of an Antarctic Dry Valley stream. Geochim. Cosmochim. Acta **66:** 1335–1347.

MCKNIGHT D. M., A. S. ALGER, C. M. TATE, G. SHUPE, AND S. A. SPAULDING. 1998. Longitudinal patterns in algal abundance and species distribution in meltwater streams in Taylor Valley, Southern Victoria Land, p. 109–127. ***In*** J. D. Priscu [Ed.], Ecosystem dynamics in a polar desert: The McMurdo Dry Valleys, Antarctica. Antarctic Research Series 72. American Geophysical Union.

———, D. K. NIYOGI, A. S. ALGER, A. BOMBLIES, P. A. CONOVITZ, AND C. M. TATE. 1999. Dry valley streams in Antarctica: Ecosystems waiting for water. Bioscience **49:** 985–995.

———, R. L. RUNKEL, C. M. TATE, J. H. DUFF, AND D. MOORHEAD. 2004. Inorganic nitrogen and phosphorous dynamics of Antarctic glacial meltwater streams as controlled by hyporheic exchange and benthic autotrophic communities. J. N. Am. Benthol. Soc. **23:** 171–188.

MULHOLLAND, P. J., A. D. STEINMAN, E. R. MARZOLF, D. R. HART, AND D. L. DEANGELIS. 1994. Effect of periphyton biomass on hydraulic characteristics and nutrient cycling in streams. Oecologia **98:** 40–47.

NEWBOLD, J. D., J. W. ELWOOD, R. V. O'NEILL, AND A. L. SHELDON. 1983. Phosphorous dynamics in a woodland stream ecosystem: A study of nutrient spiralling. Ecology **64:** 1249–1265.

NIKORA, V. I., D. G. GORING, AND B. J. F. BIGGS. 2002. Some observations of the effects of micro-organisms growing on the

bed of an open channel on the turbulence properties. J. Fluid Mech. **450:** 317–341.

POETER, E. P., AND M. C. HILL. 1998. Documentation of UCODE, A computer code for universal inverse modeling. U.S. Geological Survey Water-Resources Investigations Report 98-4080.

REYNOLDS, C. S. 2000. Hydroecology of river plankton: The role of variability in channel flow. Hydrol. Proc. **14:** 3119–3132.

RUNKEL, R. L. 1998. One-dimensional transport with inflow and storage (OTIS): A solute transport model for streams and rivers. U.S. Geological Survey Water-Resources Investigations Report 98-4018.

———, D. M. MCKNIGHT, AND E. D. ANDREWS. 1998. Analysis of transient storage subject to unsteady flow: Diel flow variation in an Antarctic stream. J. N. Am. Benthol. Soc **17:** 143–154.

SAND-JENSEN, K., AND J. R. MEBUS. 1996. Fine-scale patterns of water velocity within macrophyte patches in streams. Oikos **76:** 169–180.

SCOTT, D. T., M. N. GOOSEFF, K. E. BENCALA, AND R. L. RUNKEL. 2003. Automated calibration of a stream solute transport model: Implications for interpretation of biogeochemical parameters. J. N. Am. Benthol. Soc. **22:** 492–510.

SHEIBLEY, R. W., J. H. DUFF, A. P. JACKMAN, AND F. J. TRISKA. 2003. Inorganic nitrogen transformations in the bed of the Shingobee River, Minnesota: Integrating hydrologic and biological processes using sediment perfusion cores. Limnol Oceanogr. **48:** 1129–1140.

STIEF, P., D. DEBEER, AND D. NEUMANN. 2002. Small-scale distribution of interstitial nitrite in freshwater sediment microcosms: The role of nitrate and oxygen availability, and sediment permeability. Microbial. Ecol. **43:** 367–378.

TIEDJE, J. M., S. SIMKINS, AND P. M. GROFFMAN. 1989. Perspectives on measurement of denitrification in the field including recommended protocols for acetylene based methods. Plant Soil **114:** 261–284.

TRISKA, F. J., V. C. KENNEDY, R. J. AVANZINO, G. W. ZELLWEGER, AND K. E. BENCALA. 1989. Retention and transport of nutrients in a third-order stream in northwestern California: Hyporheic processes. Ecology **70:** 1893–1905.

VALETT, H. M., J. A. MORRICE, C. N. DAHM, AND M. E. CAMPANA. 1996. Parent lithology, surface-groundwater exchange, and nitrate retention in headwater streams. Limnol. Oceanogr. **41:** 333–345.

VINCENT, W. F., R. W. CASTENHOLZ, M. T. DOWNES, AND C. HOWARD-WILLIAMS. 1993*a*. Antarctic cyanobacteria: Light, nutrients, and photosynthesis in the microbial mat environment. J. Phycol. **29:** 745–755.

———, C. HOWARD-WILLIAMS, AND P. A. BROADY. 1993*b*. Microbial communities and processes in Antarctic flowing waters, p. 543–569. *In* Antarctic microbiology. Wiley-Liss.

WILCOCK, R. J., P. D. CHAMPION, J. W. NAGELS, AND G. F. CROCKER. 1999. The influence of aquatic macrophytes on the hydraulic and physico-chemical properties of a New Zealand lowland stream. Hydrobiologia **416:** 203–214.

Received: 19 August 2003
Accepted: 15 March 2004
Amended: 8 April 2004